Proceedings of the Second International Conference on Press-in Engineering 2021, Kochi, Japan – Matsumoto et al (eds)

A study on analysis of horizontal resistance of screw coupled foundation with vertical and battered piles in cohesionless soil

T. Kurokawa
Research and Development Center, HINODE, Ltd., Fukuoka, Japan
Department of Civil Engineering, Kyusyu University, Fukuoka, Japan

Y. Tani & M. Nagata
Research and Development Center, HINODE, Ltd., Fukuoka, Japan

A. Jugdernamjil & N. Yasufuku
Department of Civil Engineering, Kyusyu University, Fukuoka, Japan

ABSTRACT: The screw piles, made by twisting a strip of flat steel, are excellent for ease of driving and demonstrate high resistance to vertical loads. However, screw piles have a horizontal resistance is lower than that of steel pipe piles of the same diameter. In this study, the horizontal resistance of screw coupled piles, which are expected to improve, was tested by model tests in the sand tank. Based on the model test results, a static nonlinear analysis is carried out to rationalize the structural design. The analytical model was that the ground is a bilinear soil reaction spring and the pile is a beam model on the soil reaction spring. It was found out that this analysis allowed to reproduce the initial rigidity and the maximum load of the screw coupled piles structure, and an example of the optimization of the structure of vertical and battered piles was identified.

Keywords: screw pile, coupled pile, horizontal resistance, nonlinear analysis, model test

1 INTRODUCTION

The screw piles are made of flat steel twisted into a spiral shape, and are used as foundations for solar panels, sign poles and lighting columns. The spiral piles can penetrate into the ground without disturbing the surrounding ground and have high vertical resistance to vertical load (push-in and pull-out), so that small-diameter and short steel pipe piles and screw piles are being developed as a useful foundation method for soft ground. Especially in the foundation method using screw piles (Figure 1), Sato *et al.* (2014) studied the use of sand tank and ground for a more rational design. The bearing capacity characteristics were clarified by Hirata *et al.* (2005) and a bearing capacity formula was proposed and validated by elastoplastic analysis using the FEM method.

Steel screw piles are made of flat steel and have a uniform cross section. In order to optimize the shape of these piles for the external forces (moments) acting on the piles in the ground, machining is required, which is unrealistic in terms of cost. (Figure 2) is a screw pile made of ductile cast iron, allowing for shape optimization and connection to the superstructure. Kanno *et al.* (2017, 2019) have conducted test to confirm the performance of the screw piles by the driving method in a narrow area where heavy machinery is difficult to be carried in.

Ductile cast iron screw pile has already been applied as a foundation for pedestrian guard-pipes. And, it is also expected to be used as a foundation for vehicle guard-pipes, which require greater strength. Currently, design rationalization studies have also been conducted by (Wang *et al.* 2019; Tani *et al.* 2019) to determine the optimal pitch-width ratio (*pw*) for vertical bearing capacity and penetration of screw piles.

2 BACKGROUND

The horizontal resistance of screw piles is lower than that of steel pipe piles of the same diameter due to their low bending rigidity under horizontal loads. The methods to increase the horizontal resistance are to increase the pile diameter and pile length; however, there are some cases where it is difficult to do so due to manufacturing constraints and the installation environment (e.g. interference with underground

DOI: 10.1201/9781003215226-19

Figure 1. Steel screw pile (ϕ50×t12×L4200mm with a flange).

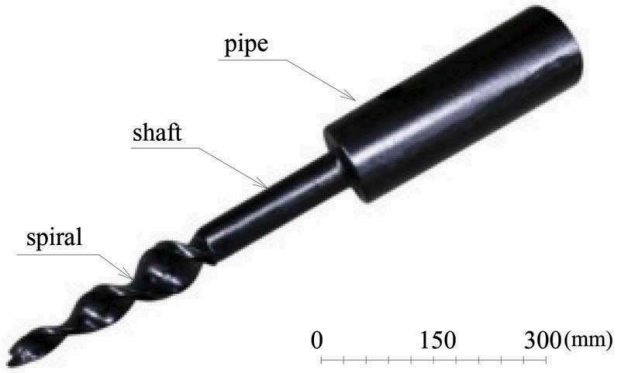

Figure 2. Ductile cast iron screw pile.

structures). The other method is to use two screw piles. The screw coupled piles are composed of vertical and battered pile, and the vertical resistance of the screw pile is utilized to improve the horizontal resistance of the structure as compared to the single pile. Tani, Amar *et al.* (2020, 2021) reported on the horizontal resistance characteristics of screw, plate and pipe single piles and screw coupled piles in an experimental sand tank and the effect of the angle of installation of battered piles. However, the rationalization of coupled pile structure design is still unclear.

In this study, the effects of the change in pile length on the horizontal resistance of vertical and battered piles were investigated by the model horizontal loading tests for rationalization of the screw coupled pile structure design. Based on the results, a static nonlinear analysis by FEM was performed to evaluate the horizontal resistance of the screw coupled piles structure by reproducing the model test and simulating full-scale.

3 HORIZONTAL LOAD MODEL PILE TESTS

3.1 *Plan of experimental*

The model test was conducted to confirm the effect of pile length change on the horizontal resistance of coupled piles. The experimental devices were the same as those used by Tani, Amra *et al.* (2020, 2021) as shown in Figure 3. The sand tanks, properties of soil medium, loading devices and instrumentation are outlined in Tables 1 to 4, and the sand tank conditions, loading conditions, and materials,

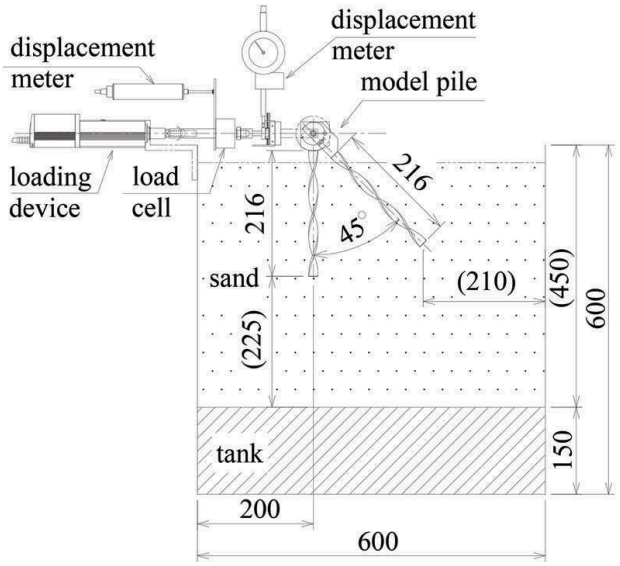

Figure 3. Experimental device.

Table 1. Sand tank.

Date	Detail	Note
Tank Size	300*600*600 (mm)	Width*Depth*Height
Sand Type	Silica Sand (K7)	Dry Sand

Table 2. Index properties of soil medium.

Properties	Value
Specific gravity, Gs	2.63
Maximum dry density, ρ_{max}	1.56 g/cm^3
Minimum dry density, ρ_{min}	1.19 g/cm^3
Coefficient of uniformity, U_c	1.76
Median diameter, D_{50}	0.17 mm
Relative density, Dr=90%	1.53 g/cm^3
Internal friction angle, °	41.9°

Table 3. Loading device.

Date	Detail
Maximum Load	800 (N)
Loading Speed	0.01 (mm/s)
Maximum Stroke	50 (mm)

Table 4. Instrumentation.

Date	Detail	Note
Load Cell	1000 (N)	
Displacement Meter	25 (mm)	Contact Type

dimensions, configuration and method of installation of the model piles are the same to compare with the existing results. The pw (pitch width ratio) of the screw piles, which affects bearing capacity and bending rigidity, was unified to 4.5.

3.2 *Model piles*

Table 5 shows the model test cases. No. 1 to 4 are for comparison with the conditions tested by Tani, Amra *et al.* (2020, 2021). Firstly, No.4 to 6 were prepared to confirm the change with the increase of the pile length in each case. In addition, the effect of the angle of the battered piles was also confirmed. Then, the effect of the structure of vertical piles and battered piles on the horizontal resistance was compared in the case of long battered piles (No.5) and long vertical piles (No.6) at an angle of 45°. The shapes of the model piles are shown in Figure 4.

3.3 *Results*

Figure 5 shows the load-horizontal displacement curves. Except for No. 6, the resistance gradually decreased with increasing displacement. No. 3 and 5 dropped to about the same level as No. 1 (144 mm single pile) and No. 4 to about the same level as No. 2 (216 mm single pile). When the load exceeded the maximum pull-out resistance of the vertical pile, the pile was pulled out. Therefore, it was assumed that the resistance was lost. The initial resistance and rigidity of No.4 was the largest, while No.6 had the largest resistance at 15mm displacement. The rigidity of No. 6 was small by the length of the battered pile. Therefore, a large amount of displacement was required before it was pulled out. The final result was estimated to be reduced to the same level. In the case of No.5, the initial rigidity of the No.5 pile was similar to that of No.6, but the resistance was lower. The results indicated that the horizontal resistance of the piles had a great effect on the pull-out resistance of vertical piles.

Table 5. Model Test Case (Pile Length, Batter Pile Angle).

No	Type	L1(mm)	L2(mm)	θ(°)
1	Single*	144	-	-
2	Single*	216	-	-
3	Coupled*	144	144	45
4	Coupled*	216	216	45
5	Coupled	144	216	45
6	Coupled	216	144	45

* Tani, Amra *et al.* (2020, 2021).

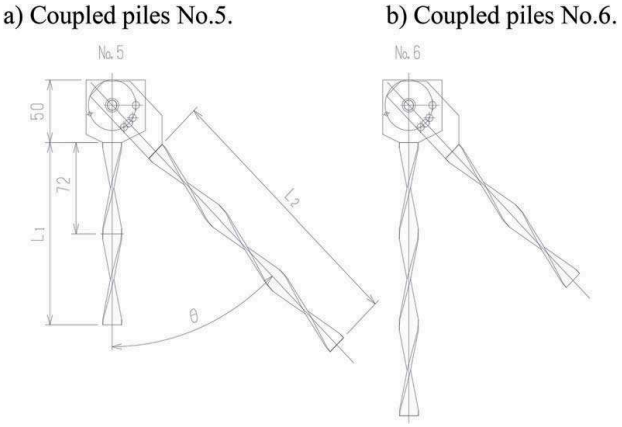

Figure 4. Model piles.

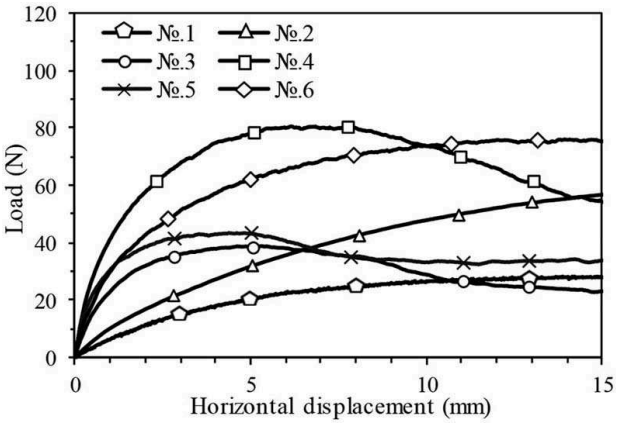

Figure 5. Load-horizontal displacement.

The ultimate bearing capacity (R_u) of a pile was the load at a displacement of 20% of the pile diameter. Figure 6 shows the results of changing the display range of the displacement amount, and Table 6 indicates the values. Also, a comparison with No. 1 and No. 3 is shown. The horizontal resistance was increased more than twice by changing from single piles to coupled piles (No.1 to No.3: 2.26, No.2 to No.4: 2.86). There was a difference of 22% in the rate of increase in resistance due to the extension of vertical and battered piles versus coupled piles. In addition, the resistance of No. 6 was still on an upward trend, while that of No. 5 had started to decrease from about 4 mm. The performance of No. 6 seems to be better.

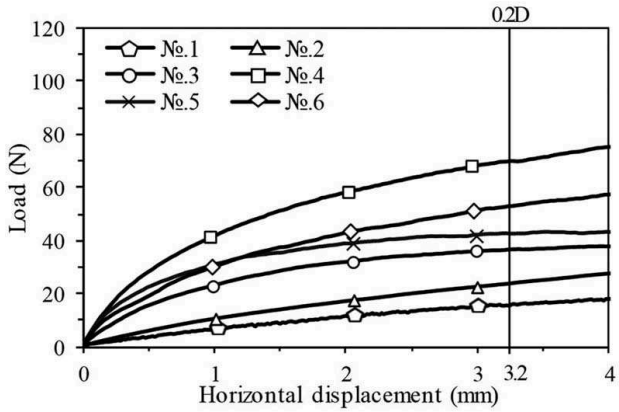

Figure 6. Load-horizontal displacement (20 % of Pile diameter).

Table 6. Ultimate horizontal bearing capacity.

No	Type	R_u (N)	Ratio No.1	Ratio No.3
1	S144	15.8	1.00	0.44
2	S216	23.6	1.49	0.66
3	V144-B144	35.8	2.26	1.00
4	V216-B216	67.4	4.25	1.88
5	V144-B216	41.9	2.65	1.17
6	V216-B144	51.2	3.23	1.43

4 STATIC NONLINEAR ANALYSIS OF HORIZONTAL LOAD TESTS OF MODEL PILES

4.1 *Analysis methods*

The results of the model test were reproduced by analysis, and the horizontal resistance was predicted under conditions that had not been tested. The same method of analysis was used as in Tani *et al.* (2020). In the analytical model, the ground was used as a non-linear soil reaction spring model with coefficients of horizontal and vertical subgrade reaction, and the pile was a beam model on the soil reaction spring, which was adjusted to the model test results. Figure 7 shows the analytical model image and Table 7 shows the boundary conditions. The pile diameter was reduced by 15% to 12 mm to match the projected area of a flat plate of the same diameter. The results of the four-point bending test of flat plates and spirals in air conducted by the authors (2020) revealed the relationship between the bending rigidity EI (E: Young's modulus, I: Moment of inertia of area) of a spiral, and Amar *et al.* (2021) proposed a formula for calculating it. The I of the spiral was found to be I=102(mm^4). From these results, the dimensions of the analytical model were determined to be w=12mm and t=4.68mm. Table 8 shows the material properties of the pile body and Table 9 shows the dimension properties of the pile body. The pile body was treated as a linear material since it was rigid enough against sand.

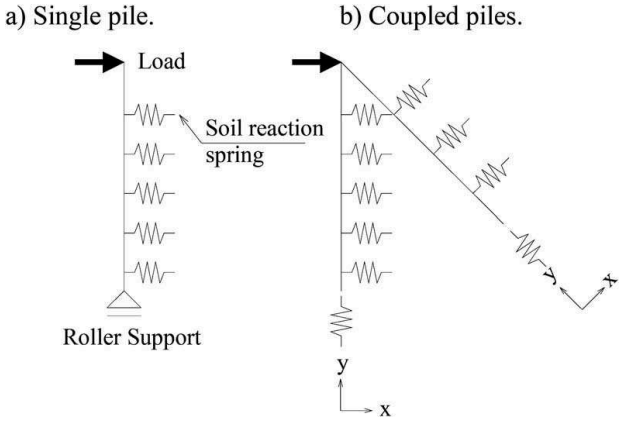

Figure 7. Soil reaction spring model.

Table 7. Fixed constraint.

Single				Coupled			
Displacement		Rotation		Displacement		Rotation	
X	free	X	fix	X	free	X	fix
Y	fix	Y	fix	Y	free	Y	fix
Z	fix	Z	free	Z	fix	Z	free

4.2 *Estimation of horizontal subgrade reaction coefficient and deformation modulus for sand tanks*

The horizontal subgrade reaction coefficient kh_0, which was the initial rigidity of the soil reaction spring, was calculated from the formula 1 according to the "Specifications for Highway Bridges, 2017 (Japan Road Association)".

$$kh_0 = \alpha \cdot \frac{E_0}{0.3} \tag{1}$$

E_0 : deformation modulus
α : conversion factor

Otake *et al.* (2017) reported a method for estimating soil deformation modulus for design. E_1 (deformation modulus at axial strain ε_a=0.01(1%) is called the base deformation modulus. This corresponds to the average value of E_{50} (deformation modulus calculated from 1/2 of the maximum principal stress difference in the triaxial compression test and the slope

Table 8. Material properties.

Date	Value	Note
E (GPa)	200	Yong's modulus
ν	0.3	Poisson's ratio

Table 9. Dimension properties.

Date	Actual size	Analysis size	Ratio
w (mm)	16	12	0.75
t (mm)	3	4.68	1.56
I (mm^4)	36	102	2.83

w : Width
t : Thickness
I : Moment of inertia of area $(I = w \cdot t^3/12)$

from the zero point). From this, the deformation modulus can be estimated for an arbitrary axial strain.

The results of the triaxial compression test of the sand used in this study are indicated in Figure 8. E_{50} and E_1 were plotted for each of the axial stresses in Figure 9, and the respective approximate equations were obtained. The soil pressure applied to the pile was calculated from

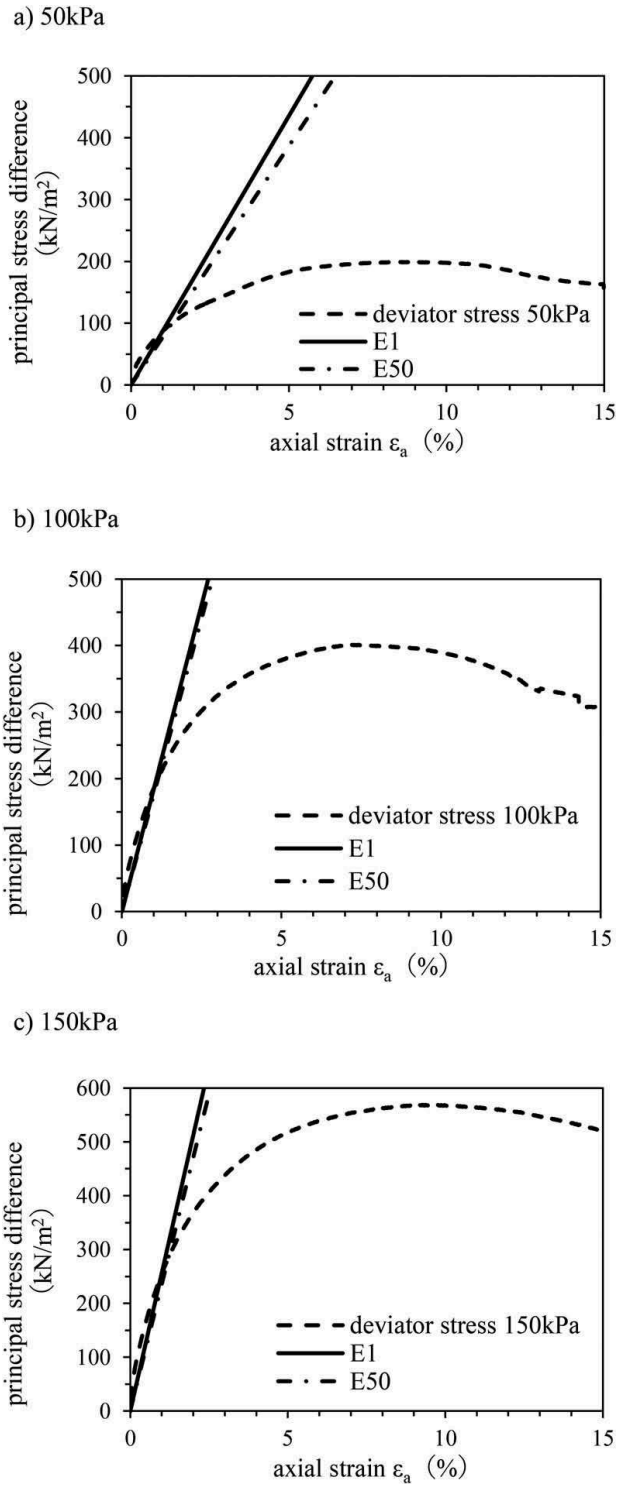

Figure 8. Triaxial compression test.

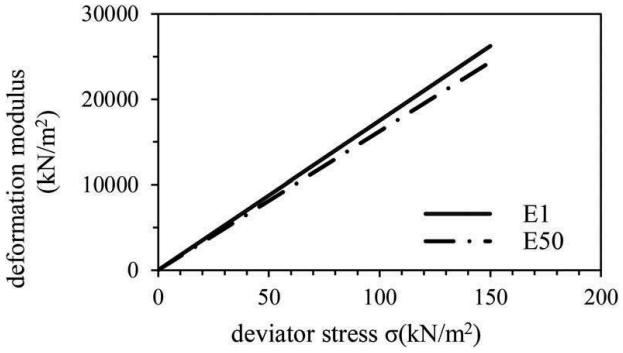

Figure 9. Deformation modulus.

the installation depth of the pile and the unit volume weight of sand in the model test, and the deformation modulus was obtained from the approximate equation of E_{50}. In this study, the approximate equation of E_{50} was adopted because the design was made on the safety side. The value of α was 4 when the deformation modulus was obtained from the triaxial compression test. The horizontal subgrade reaction coefficient was estimated from these. The specific procedure for setting the soil reaction springs is described below.

- Setting procedure for bilinear soil reaction springs.
  - I. Setting the number of springs.
    The mesh size was divided into 20 segments for a pile length of 144 mm and 30 segments for a pile length of 216 mm. One spring per two meshes is set.
  - II. Calculation of coefficient of passive earth pressure.Calculated from Coulomb's formula 2.

$$K_p = tan^2\left(45° + \frac{\phi}{2}\right) \quad (2)$$

ϕ : Internal friction angle, 41.9°
(from triaxial compression test)

  - III. Setting of passive soil pressure (maximum spring force).
    Calculated from Coulomb's formula 3. The passive soil pressure (kN/m^2) is calculated by multiplying the passive earth pressure (kN/m^2) by the mesh area (m^2, pile diameter x spring spacing) and this is the maximum spring force. According to Blombs (1964), there is a difference between the calculated and measured passive soil pressure, and correction is required. The correction factor (CF) varies depending on the ground conditions. In this analysis, corrections were made to the calculated passive soil pressure values and adjusted with the model tests.

$$P_p = K_p \cdot \gamma \cdot z \quad (3)$$

γ : unit weight, 15.3(kN/m^3)
z : Installation depth of the spring (m) (optional)

IV. Setting of spring rigidity.
The coefficient of horizontal subgrade reaction (kN/m^3) is multiplied by the mesh area (m^2) to calculate the spring rigidity (kN/m).

V. Setting of displacement at the maximum spring force.
The displacement is calculated by dividing the maximum spring force (kN) by the spring stiffness (kN/m).
This is the displacement to reach the maximum spring force.

VI. Setting of bilinear soil reaction springs.
The bilinear soil reaction spring is obtained from the spring rigidity, the maximum spring force and the displacement. Since the maximum spring force depends on the depth of the spring, set the spring for each position. Figure 10.

4.3 *Estimation of axial soil reaction springs of sand tank*

Next, the axial spring was set up to reproduce the bearing capacity of the pile to compress and pull-out the pile. The vertical bearing capacity of a screw pile consists of the frictional force acting on the circular area of the pile body, which is determined from the shear force of the sand. However, in practice, it is assumed that soil getting into the twisting part of the screw pile would also add physical resistance, which would result in greater bearing capacity than this, but the detailed mechanism is not clear.

In this study, model tests were carried out to estimate the vertical bearing capacity and pull-out resistance of the screw pile. The test conditions and other details were identical to those reported by Tani, Wang *et al.* (2019). Screw piles of 25 and 44 widths with different pile diameters from the present tests were used for the model piles. Later, an empirical equation was obtained to allow estimation of the pile diameter and sand conditions as they changed (pw=4.5 is fixed). The results are shown in Figures 11 and 12. As the pile diameter increased, both resistances increased. In contrast to the horizontal resistance, the displacement did not progress almost at the beginning of loading, but gradually increased from a certain point to the maximum level. In the pull-out test, the resistance force decreased after reaching the maximum value. From the results, the axial soil reaction springs of this test is estimated. Based on the behavior of the test results and the analysis time, the trilinear type was set up in this study. Setting up a multilinear type seems to improve the accuracy more. The specific procedure for setting the springs is described below.

- Setting procedure for trilinear soil reaction springs.
  I. Non-dimensionality of model test results (w25 and w44).
  Figures 11 and 12 shows the result of bearing capacity divided by circumference area and displacement divided by pile diameter. In both cases, the tendency was almost the same at w25 and w44, and it was confirmed

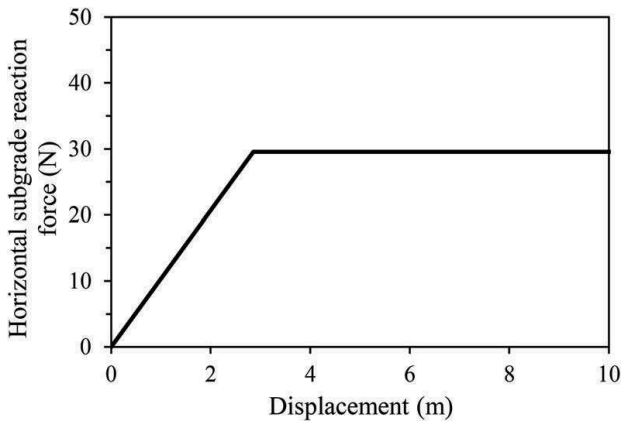

Figure 10. Bilinear soil reaction springs. (Example of a 216mm coupled piles 45deg).

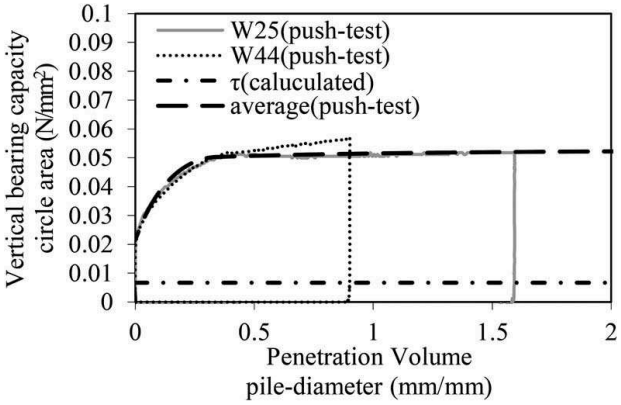

Figure 11. Static axial compressive load model test.

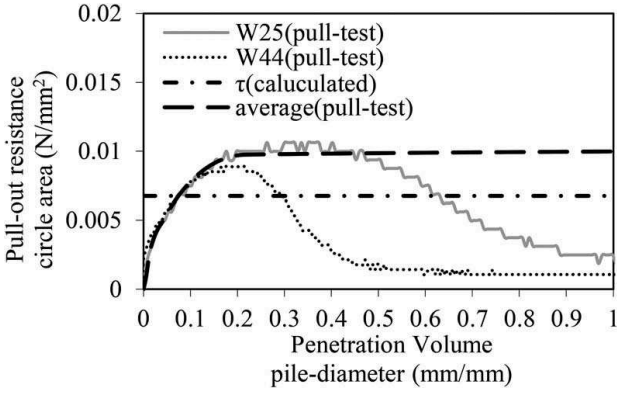

Figure 12. Axial tensile load model test.

that the bearing capacity depended on the pile size.

II. Calculation of the shear strength of sand (compressive, pull-out model test) and estimation of correction factors.
The shear strength of the sand in the tank was calculated from the following formula. The difference between the calculated value and the test results (Figures 11 and 12) was confirmed, and the correction factor was determined by the shape of the screw pile.

$$\tau = c + \sigma tan\phi \quad (4)$$

c : cohesion, 0
σ : earth pressure at rest (normal stress)
ϕ : 41.1° (From Kang et al. 2019 test results, sand type: K7, relative density: 75%)

$$\sigma = \sigma_c + K_0 \cdot \gamma \cdot z \quad (5)$$

σ_c : overburden pressure, 12.6(kN/m^2)
K_0 : coefficient earth pressure at rest, 0.5
γ : 14.3(kN/m^3)
z : 0.7(m)

III. Calculation of the shear strength of sand (This horizontal load model test).
The bearing capacity of the horizontal load model test was calculated using the above equations and correction factors. The sand tank conditions and model pile conditions were changed (ϕ =41.9°, σ_c=0, D_r=90%, γ=15.3(kN/m^3), z : optional) and reflected in the calculations. Figures 13 and 14 show the average values of the model tests and the calculated values (with and without overburden pressure).

IV. Setting of trilinear soil reaction springs.
From these, the trilinear soil reaction spring was set up that connecting the zero-point, linear elastic range, and maximum value. The vertical and battered piles were set axially at their respective ends. An example is shown in Figure 15.

4.4 *Analysis cases*

The analysis cases are shown in Table 10. Firstly, No.1 to No.5 were analyzed in order to check the consistency with the model tests. Amar *et al.* (2021) reported that resistance increases at 45-60 degrees of battered pile angle. The analysis of No. 6 to 9 was conducted with the battered pile angle as a change parameter. The horizontal resistance of the battered pile angle is determined by the analysis.

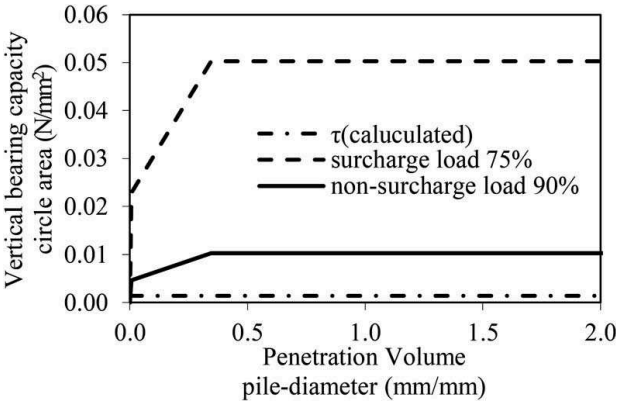

Figure 13. Static axial compressive load - non-dimensionless.

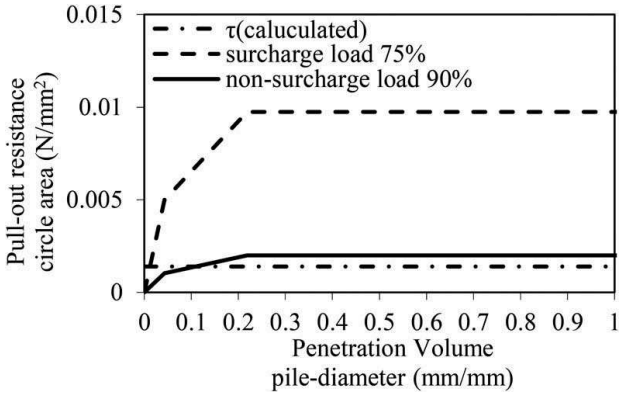

Figure 14. Axial tensile load - non-dimensionless.

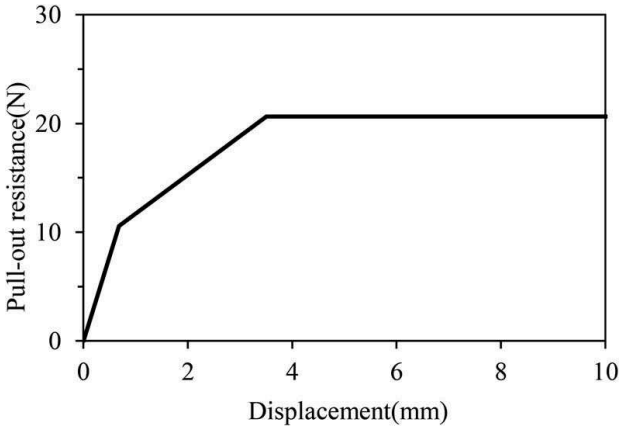

Figure 15. Trilinear pull-out soil reaction springs. (Example of a216mm vertical pile).

4.5 *Results*

The results are indicated in Figure 16 together with the results of the model tests. By adjusting the *CF* for the maximum horizontal soil reaction springs, the results of the analysis are close to the test results. The correction factor was set to 30 for No. 1 and 3,

Table 10. Model test case (Pile Length, Batter Pile Angle).

No	Type	L1(mm)	L2(mm)	θ(°)
1	Single	144	-	-
2	Single	216	-	-
3	Coupled	144	144	45
4	Coupled	216	216	45
5	Coupled	216	144	45
6	Coupled	216	216	50
7	Coupled	216	216	55
8	Coupled	216	216	60
9	Coupled	216	216	70

and 12 for all other cases, depending on the length of the vertical pile. Table 11 shows the difference between the ultimate bearing capacity and the model test, as well as the difference in the battered pile angle.

The error of the ultimate bearing capacity was less than 8% for No. 1 to No. 4 and 14% for No. 5. It is assumed that the correction factors will vary with the pile structure and ground conditions. The accuracy of the analysis would be improved if it is possible to set the correction factors for each case. However, more elemental experiments are needed to organize the correction factors logically and systematically. The load-displacement curves generally reproduced the trends of the model tests. This was made possible by setting up two types of nonlinear soil reaction springs.

Next, it was found that the horizontal resistance decreased gradually as the angle of the battered piles became larger than 45°. It is assumed that this is due to the shallow installation depth of the battered piles. However, the initial rigidity is higher at larger angles (Figure 16-g). It is assumed that this is because the axial spring of the battered pile is more likely to contribute to the horizontal resistance. It is necessary to investigate the optimum angle of the battered piles by unifying the installation depth of the battered piles and varying the angle of the piles.

In the case of coupled piles, some deviation was observed in the initial stage. It is assumed that this is due to the non-dimensionality of the estimation by setting the springs and so on. In this study, only the range of small displacement (about 25% of the pile diameter) was focused on, but it seems that the setting of the spring in the axial direction will make it possible to predict the deformation in a larger range.

5 STATIC NONLINEAR ANALYSIS OF PRODUCTS IN COHESIONLESS SOIL

5.1 *Outline of analysis*

Based on the previous model tests and analysis results, a study on the full-scale screw coupled pile foundations

a) No.1 Single pile 144. *CF*=30.

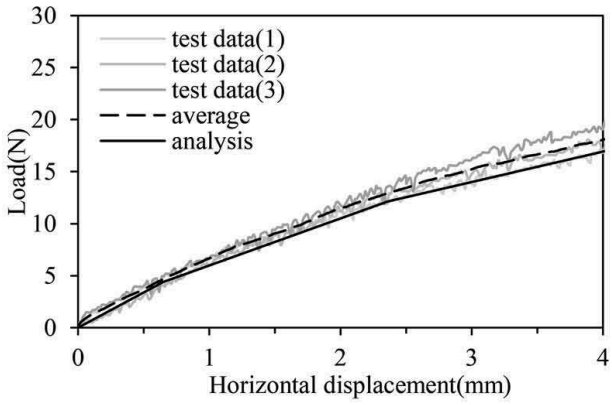

b) No.2 Single pile 216. *CF*=12.

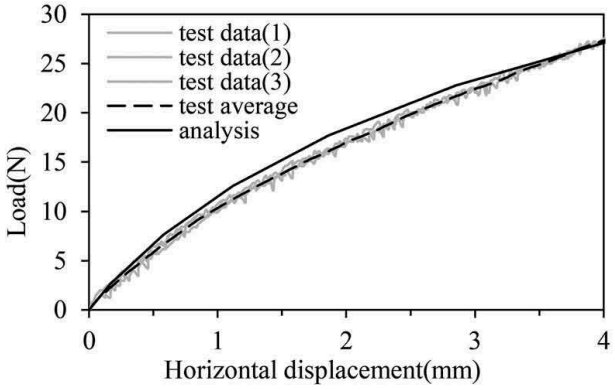

c) No.3 V144-B144. *CF*=30.

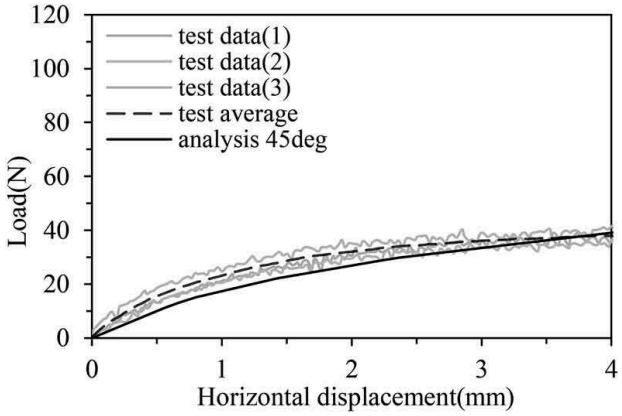

d) No.4 V216-B216-45deg. *CF*=12.

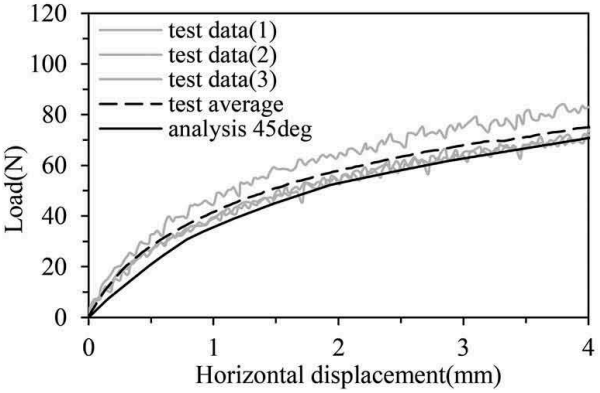

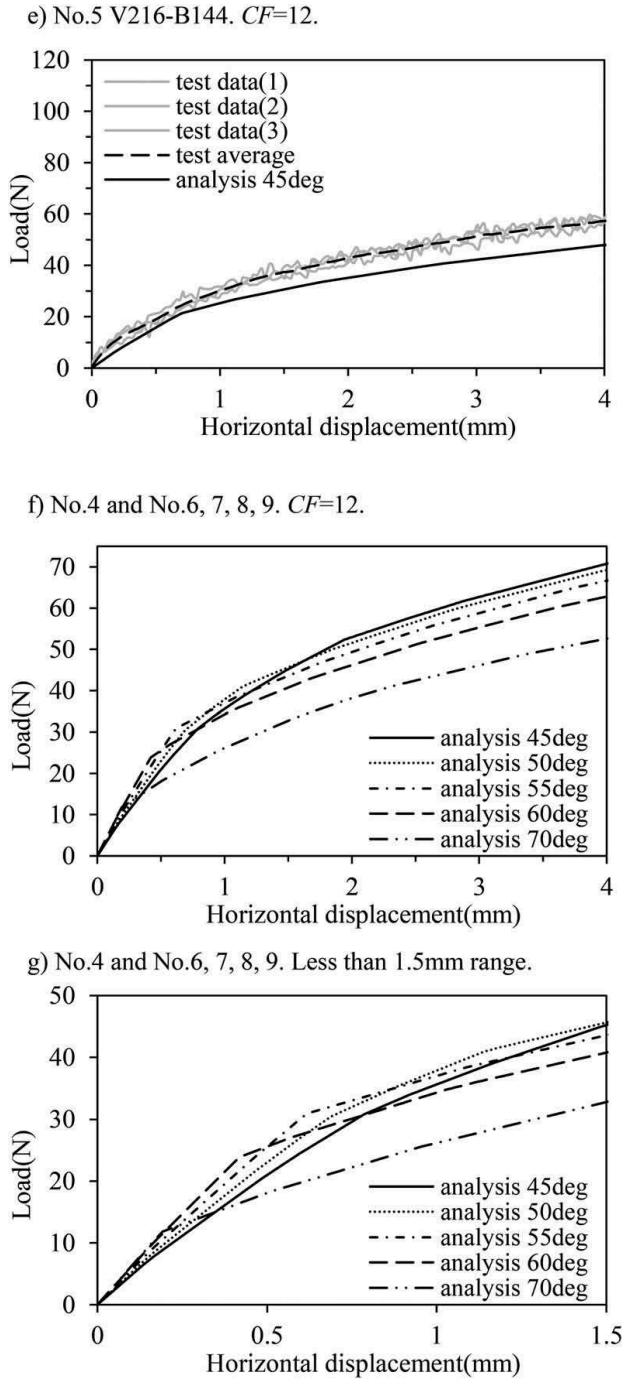

Figure 16. Load-horizontal displacement analysis.

was conducted. From "Standard Specifications of Vehicle Guard-pipe, 2014 (Japan Road Association)", a steel pipe pile ϕ114.3×t4.5mm×L1500mm was used as a comparison target for a foundation for a vehicle guard-pipe. In contrast, a foundation with a screw coupled pile angle of 45° was devised and analyzed. The screw piles were constructed with a tubular part and a spiral part is shown in Figure 17 with referring to the ductile cast iron pile structure shown in Figure 2. The vertical piles, the tubular part was ϕ114.3×t4.5×L_p =400mm, the spiral part was w150×t28×L_s=350, 600, 850, 1100mm, and the total length was L=750, 1000, 1250, 1500mm. The battered piles, tubular part was ϕ114.3×t4.5×L_p=150mm, the spiral part was w150×t28×L_s=350mm, and the total length was L=500mm. The analysis of vertical pile only (L=1500mm) was also performed for comparison. The analysis cases were shown in Table 12 and the analysis model was shown in Figure 18. The tube is provided to ensure strength and to connect to the superstructure. Vertical piles and battered piles were connected with rigid beam elements at the pile head to be integrated. The piles and the guard-pipe poles were connected at the pile head and horizontal loads were applied to the poles.

The coefficients of horizontal subgrade reaction force and the deformation modulus were based on the values obtained for the sand tank condition in the

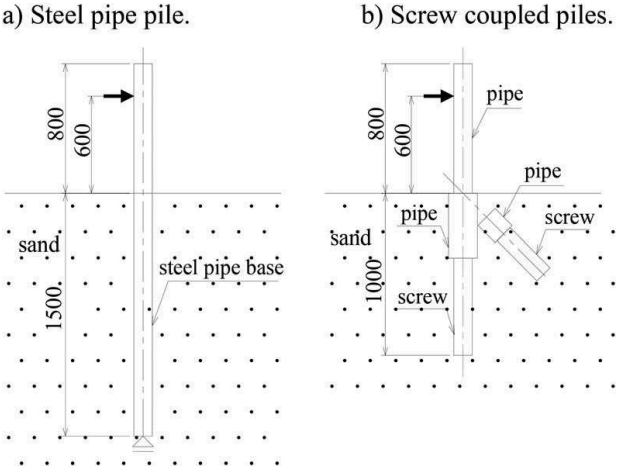

Figure 17. Piles foundation.

Table 11. Ultimate horizontal bearing capacity.

No	1	2	3	4	5
Model test	15.8	23.6	35.8	67.4	51.2
Analysis	14.6	24.1	35.0	65.2	44.2
Ratio test	0.92	1.02	0.98	0.97	0.86
No	6	7	8	9	
Model test	64.0	61.6	58.2	48.4	
Ratio No.4	0.98	0.95	0.89	0.74	

Table 12. Analysis Cases (Pile Length, Spiral part Length).

No	Type		L(mm)	L_p(mm)	L_s(mm)
1	Single	Pipe	1500	1500	-
2	Single	Screw	1500	400	1100
3	Coupled	Screw	1500	400	1100
4	Coupled	Screw	1250	400	850
5	Coupled	Screw	1000	400	600
6	Coupled	Screw	750	400	350

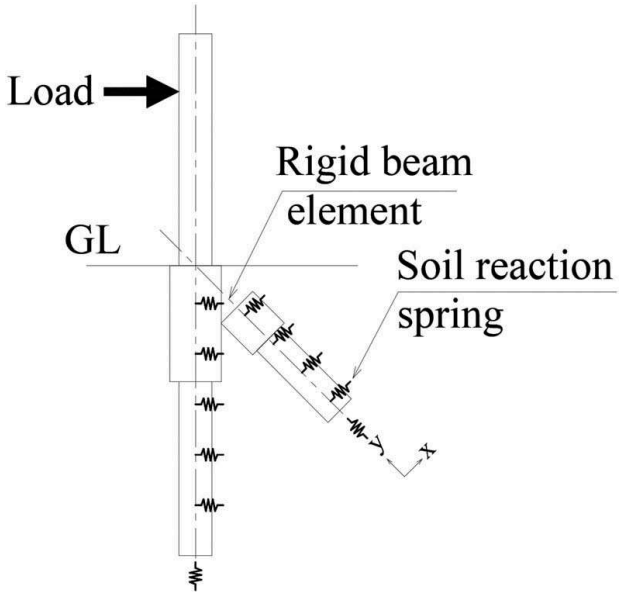

Figure 18. Analytical model.

previous chapter. The axial soil reaction springs was estimated from the results of the pull-out test conducted in the field. Otake *et al*. 2017 also discussed the case of estimating the design deformation modulus from the *N* value. In practice, it was also important to estimate from the *N* value. However, they reported that there is no data for the surface layer less than 2.5m, and setting the deformation modulus for the surface layer, such as the assumption in this case, is an important issue, which was not clear.

5.2 *Results*

The load-horizontal displacement curves were shown in Figure 19. *CF* for passive earth pressure were assumed to be 12. The rigidity of the vertical pile alone was inferior to that of the steel pipe pile due to the presence of the spiral parts. The rigidity and horizontal resistance of the coupled piles were higher than those of the steel pipe piles in No. 3, 4 and 5. The range of displacements less than 30 mm is shown in Figure 20. The ultimate horizontal bearing capacity was compared. The initial rigidity of

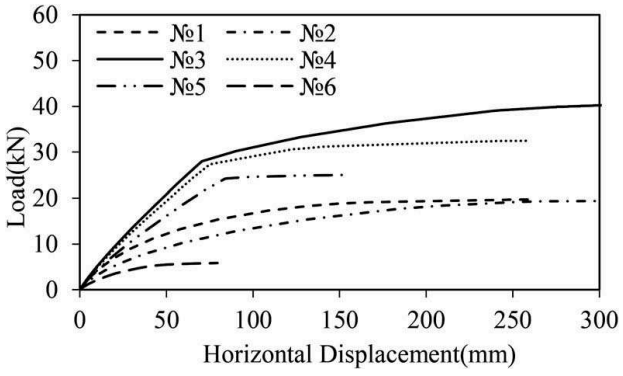

Figure 19. Load-horizontal displacement analysis.

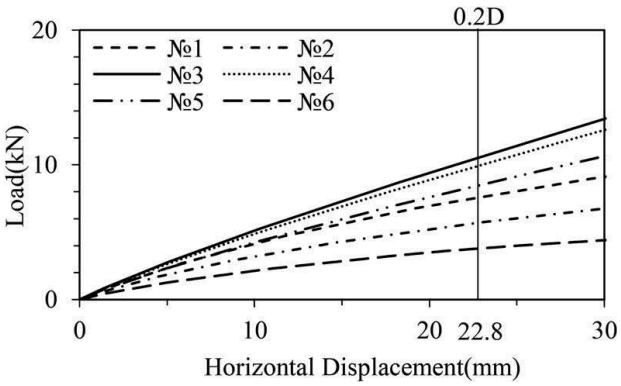

Figure 20. Load-horizontal displacement analysis (20% of Pile diameter).

No. 5 was almost the same as that of the steel pipe pile, and the ultimate horizontal bearing capacity was a little higher, about 1.1 times. In the future, it is necessary to investigate the stresses in the pile body, the manufacturability, the connection between vertical and diagonal piles, and the constructability of the pile. In addition, we would like to reproduce the behavior of the loss of pull-out resistance of vertical piles, rationally set the correction factor for the passive earth pressure (upper limit of spring), the influence of pile length in setting the axial soil reaction springs of screw piles, and confirm the validity by experiments on field. This will improve the accuracy of analysis and enable more rational design.

6 CONCLUSION

- A study was carried out to clarify the relationship between the screw coupled pile structure and the horizontal resistance force in cohesionless soil through model tests and FEM analysis. Next, FEM analysis was carried out on a full-scale in order to propose a practical coupled pile foundation.
- Based on the properties of soil medium and the results of previous model tests, horizontal subgrade reaction coefficients, deformation modulus, and axial soil reaction springs in the sand tank were determined to provide a sufficiently accurate FEM analysis.
- From this, we obtained a proposal for the structure of coupled piles with the same performance as steel pipe piles.

ACKNOWLEDGEMENTS

In this study, we would like to acknowledge Mr. M, Nakajima and Mr. Wang, K. technical staff, for their technical support and cooperation.

REFERENCES

Amarbayar, J., Yasufuku, N., Ishikura, R., Tani, Y., Nagata, M. & Kurokawa, T. 2020. *Experimental Studies on Behavior of Screw Vertical-Batter Pile Under Lateral Loading in Sand*. The 55th Geotechnical Research Presentation, online.

Amarbayar, J., Yasufuku, N., Ishikura, R., Tani, Y., Nagata, M. & Kurokawa, T. 2021. *Experimental Observation on Behavior of Ultimate Lateral Capacity of Vertical-Batter Screw Pile Under Monotonic Loading in Cohesionless Soil*. The Second International Conference on Press-in Engineering 2021, Kochi (submitting a paper).

Broms, B, B., 1964. *Lateral Resistance of Piles in Cohesionless Soils*. Journal of the soil mechanics and foundations division. Proceedings of the American Society of Civil Engineers. May, 1964.

Hirata, A., Kokaji, S., Kang, S, S. & Goto, T. 2005. Study on the *Estimation of Axial Resistance of Spiral Bar Based on Interaction with Ground*. Shigen-to-Sozai, Vol.121, No.8.

Kang, J. G., Yasufuku, N., Ishikura, R., & Purama, A. Y. 2019. *Prediction of Uplift Capacity of Belled-type Pile with Shallow Foundation in Sandy Ground*. Lowland Technology International 2019; 21 (2): 71–79.

Kanno, T. & Muraoka, H. 2017. *Traffic Safety Facility Foundations for Community Roads*. The 32th Japan Road Conference, Tokyo.

Kanno, T. & Kurokawa, T. 2019. *Study of Foundation Screw Piles for Guard-Pipes, Vehicle Stops, etc. for Community Roads*. The 33th Japan Road Conference, Tokyo.

Kurokawa, T., Tani, Y., Nagata, M. & Nagasaki, R. 2020. *Tension and Four-Point Bending Test of Spiral Piles (Twisting a Strip Flat Steel*). The 55th Geotechnical Research Presentation, online.

Otake, Y., Nanazawa, Y., Honjo, Y., Kono, T. & Tanabe, A. 2017. *Improvement of Deformation Modulus Estimation Considering Soil Investigation Types and Strain Level*. Journal of JSCE C, Vol. 73, No. 4, 396–411.

Purama, A, Y., Yasufuku, N. & Ahmad, R. 2019. *Evaluation of Filler Material Behavior in Pre-Bored Pile Foundation System due to Slow Cyclic Lateral Loading in Sandy Soil*. International Journal of Geomate, June 2019, Vol.16, 58, pp.90–96.

Sato, T., Harada, T., Iwasa, N., Hayashi, S. & Otani, J. 2010. *Effect of Shaft Rotation of Spiral Piles Under its Installation on Vertical Bearing Capacity.* Japanese Geotechnical Journal, Vol. 10, No. 2, 253–265.

Tani, Y., Wang, K., Yasufuku N., Ishikura, R., Fujimoto, H. & Nagata, M. 2019. *Model Test for Bearing Capacity of Spiral Pile in Sandy Ground Focused on Pitch-Width Ratio*. The 54th Geotechnical Research Presentation, Saitama.

Tani, Y., Amarbayar, J., Yasufuku N., Ishikura, R., Kurokawa, T. & Nagata, M. 2020. *Horizontal Loading Test of Spiral Piles in Sand*. The 55th Geotechnical Research Presentation, online.

Wang, K., Tani, Y., Yasufuku N., Ishikura, R., Fujimoto, H. & Nagata, M. 2019. *Bearing Capacity Characteristics of Spiral Pile in Sandy Ground Focused on Pitch-Width Ratio*. The 54th Geotechnical Research Presentation, Saitama.

Yamagata, K., Ito, A., Yamada, T. & Tanaka, T. 1991. *Statistical Study on Ultimate Point Lord and Point Load Settlement Characteristics of Cast-in-Place Concrete Piles*. Journal of Struct. Constr. Engng, AIJ, No 423, May.

Yamagata, K., Ito, A., Tanaka, T. & Kuramoto, Y. 1992. Statistical Study on Ultimate Point Lord and Point Load Settlement Characteristics of Bored Precast Piles. Journal of Struct. Constr. Engng, AIJ, No 436, June.